Influence of "Controlled Processing Conditions" on the Solidification of iPP, PET and PA6

Vincenzo La Carrubba (1), Valerio Brucato (2), Stefano Piccarolo (1)*

(1) D.I.C.P.M., University of Palermo, Viale delle Scienze, 90128, Palermo, Italy
(2) D.I.C.A., University of Salerno, Via Ponte don Melillo, 84084 Fisciano (SA), Italy

Summary: In this work reliable experimental data for three semicrystalline polymers (iPP, PA6, PET) crystallised under pressure and high cooling rates are supplied. These results were achieved on the basis of a model experiment where drastic "controlled" solidification conditions are applied. The final objective was to quantify the effect of two typical operating conditions (pressure and cooling rate) on the final properties and morphology of the obtained product. The influence of processing conditions on some macroscopically relevant properties, such as density and micro hardness is stressed, together with the influence of processing conditions on the product morphology, investigated by means of Wide Angle X-Ray Scattering (WAXS).
Results on the iPP samples display a decrease of density and micro hardness, due to the pressure increase, in a wide range of cooling rates (from 0.01 to 20 °C/s). PET samples exhibit an opposite behaviour with density and micro hardness increasing at higher pressures in the whole range of cooling rates investigated. PA6 samples behave similarly to PET displaying a less significant increase of density and micro hardness with pressure than PET samples.

1. Introduction

Solidification process in the most widely employed industrial processes is a complex phenomenon where flow fields, high thermal gradients and high pressures determine the final morphology and the resulting properties. Due to the experimental difficulties, any investigation of polymeric structure dependence upon pressure and cooling rate has been mainly performed using conventional techniques, such as dilatometry and differential scanning calorimetry under isothermal conditions or non isothermal conditions but at cooling rates several orders of magnitude lower than those experienced in industrial processes.

The complexity of the study is far higher if the behaviour of a semicrystalline polymer is investigated, since the lack of information on the influence of processing conditions on crystallization kinetics restricts the possibilities of modelling and simulating the

 CCC 1022-1360/00/$ 17.50+.50/0

industrial material transformation processes. The development of a model able to describe polymer behaviour under drastic solidification conditions is a goal very far to be achieved standing the actual background. Therefore a possible approach, along this general framework, consists in designing and setting-up model experiments with the aim to isolate and study the influence of some experimental variables on the final properties and on the final morphology. Thus a systematic investigation on polymer solidification under processing conditions should start on the separate study of the influence of flow, pressure and temperature on crystallization kinetics. In the past few years many researches have been devoted to determine how the final properties of a product depend upon cooling rate, that represents the most relevant parameter governing the polymer solidification. In the last few years a special equipment has been developed and widely tested in order to quench polymeric samples in a wide range of experimental conditions up to very high cooling rates (up to 2000 °C/s) under quiescent conditions: it has been possible to collect many information about the influence of cooling rate on the final properties of some widely used polymer, such as iPP, PET, PA6 [1-6].

The aim of the present investigation is to highlight the dependence of the final property distribution (in terms of mechanical properties, volumetric properties and final morphology) upon the experimental conditions adopted throughout the solidification. A model experiment able to achieve these goals under controlled conditions was designed, set-up and optimised in our laboratory. The methodological approach of recording the thermal histories of samples cooled under pressure and then analysing the resulting morphology and properties was adopted. All the available data concerning polymer crystallization under very high cooling rates at ambient pressure were extensively used as a starting point to evaluate the effect of pressure when superimposed to the one of cooling rate. Then non-isothermal crystallization behaviour was then determined as function of the applied pressure [7-9].

In order to generalise the results achievable with the help of this proposed experimental approach, three different polymers that covers a large variety of application fields has been adopted: isotactic PolyPropylene (iPP), PolyEthyleneTerephtalate (PET) and PolyAmmide6 (PA6). The study of three very different polymers, as far as their chemical and physical features are concerned, could be helpful for successive modelling of polymer behaviour during crystallization under processing conditions.

2. Experimental Part

For the purpose of our work an injection moulding iPP grade named "T30G" kindly supplied by Himont was employed, having the following main features: M_n = 75100; M_W = 483000; M_W / M_n = 6.4. PET was kindly supplied by SINCO. It is named "base PET" and its intrinsic viscosity is equal to 0.62 dl/g. PA6, kindly supplied by DSM, was characterized by M_W=25000, M_n =13000.

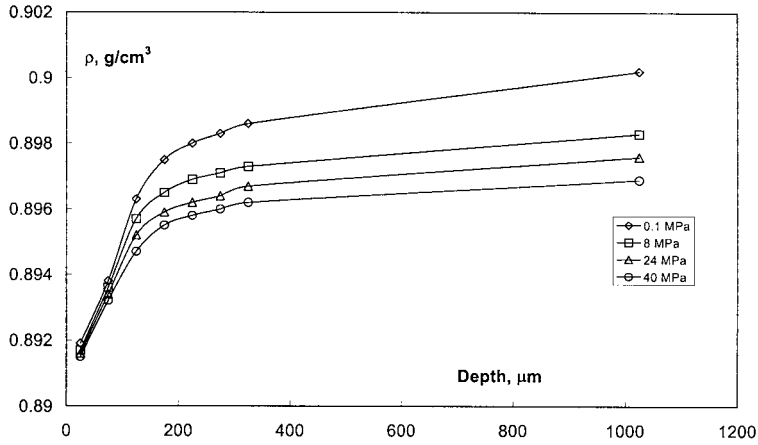

Fig. 1. Density depth profile for iPP (diaphragm 3.5 mm thick)

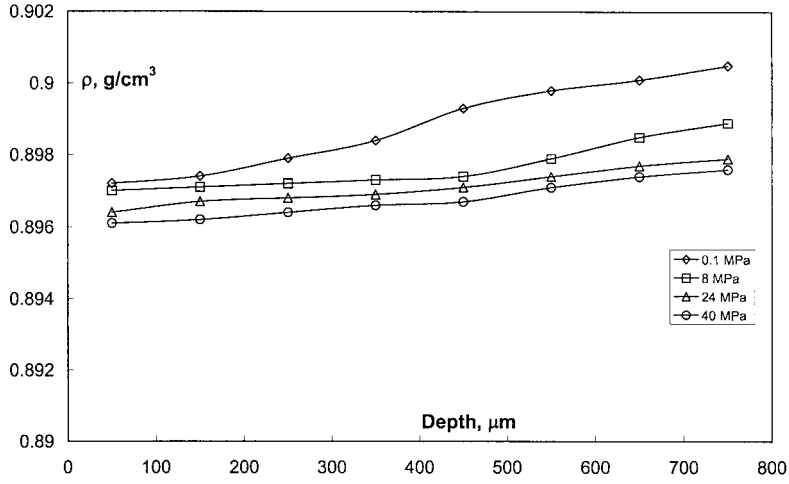

Fig. 2. Density depth profile for iPP (diaphragm 8 mm thick)

Materials were quenched under pressure and high cooling rates according to a procedure already reported [7-11]. The basic idea was to set up a model experiment where to couple rapid cooling histories with pressure levels up to 40 MPa under controlled conditions. The experimental apparatus consisted of a modified injection moulding machine, used as a source of molten polymer supplied at a pre determinable and maintainable constant pressure [7-8]. Another apparatus was used for crystallizing iPP samples at low cooling rates, consisting in a pressurized cell where the polymer was confined and maintained under hydrostatic pressure [9].

Prepared samples were subjected to the following characterization techniques: density measurements, Wide-angle X-ray Scattering (WAXS), Micro Hardness measurements. A deconvolution technique on iPP and PA6 WAXS patterns was applied to evaluate the final phase content of samples, according to a procedure reported elsewhere [12].

3. Results and Discussion

3.1 Density and micro hardness results on iPP samples

Results of density measurements on iPP samples are reported in figs. 1-2. Four different pressure conditions have been explored: 0.1 MPa, 8 MPa, 24 MPa, 40 MPa and two different diaphragms, 3.5 mm and 8 thick respectively. In fig. 1 the density depth profile for the 3.5 mm thick diaphragm is reported, whereas in fig. 2 the density depth profile for the 8 mm thick diaphragm is shown. Samples obtained with the 3.5 mm thick diaphragm are characterized by a surface cooling rate (at 70°C) of about 100°C/s; samples solidified using the 8 mm thick diaphragm have a surface cooling rate of about 20°C/s at 70°C. The cooling rates

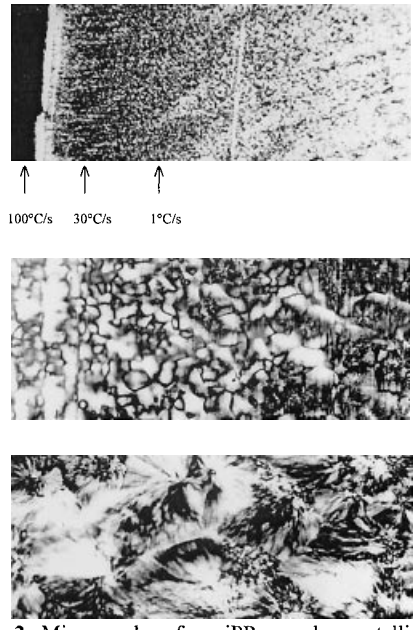

Fig. 3. Micrographs of an iPP sample crystallized under pressure with different magnifications: a) variation of structure with depth (100X); b) negative spherulites in the superficial zone (250X); c) mixed spherulites in the internal zone (250X).

have been evaluated at 70°C since it has been shown by several previous work in this field that the cooling rate calculated at 70°C is a good measure of quench effectiveness [1-2]. It is worth noticing that a diaphragm thickness corresponds to a superficial cooling rate since the diaphragm acts as a "thermal insulated body" [7-9].

Figs. 1 and 2 show that in both experiments, for all pressure values, density is increasing proceeding from the surface to the bulk of the sample. This behaviour can be related to an increase of crystallinity considered that the internal slices are cooled at lower rates. In other words, internal layers of the polymer undergo a less severe quenching and hence a larger crystallinity develops giving rise to a larger density. In figs. 1 and 2 the largest part of the density increase takes place in the neighborough of the surface and this is independent on the applied pressure. This is qualitatively confirmed by the micrographs shown in fig. 3 a) where the significant changes of the formed structure are localised near the surface in a layer of about 400 μm. It is also worth noting that we find negative spherulites near the cooled wall [fig. 3 b)], whereas inside the sample there is the typical spherulitical structure characterized by mixed spherulites. [fig. 3 c)]. Negative spherulites have a greater birefringence than mixed spherulites of the internal sample zone, depending upon the higher cooling rates experienced by the initial sample layers.

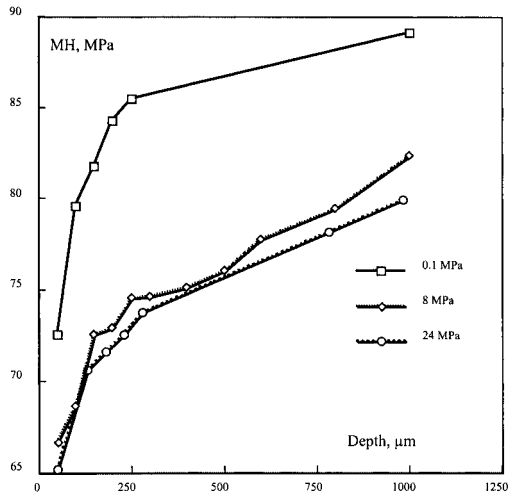

Fig. 4. Micro Hardness depth profile for iPP

Both figs. 1 and 2 show the same somewhat unexpected result: as a matter of fact density decreases when pressure increases at the same depth. The decrease in the density by effect of pressure is minimum at the sample surface and grows with depth. Furthermore, the majority of the density change is observed by varying the pressure from 0.1 to 8 MPa, this value being quite low especially if compared to the typical pressure values attained in polymer processing. This experimental result may be of

relevance for modelling shrinkage and internal stresses distribution in injection moulding; particularly important is the fact that this outcome is more pronounced in the bulk of the sample [13-15].

In fig. 4 micro hardness measured along the depth on a transverse section versus depth is reported. The same dependence on pressure as density is observed, although the curves at pressures above 8 MPa collapse on each other, which is also relevant for process simulation especially with reference to mechanical properties.

As a matter of fact also from fig. 1 and 2 it is worth noticing that on increasing pressure density curves tend to level off. Additionally, the greatest density differences are in the internal zones of the samples, which are subjected to the lowest cooling rates. Going from the surface towards the bulk of the sample (i.e. decreasing the cooling rate) the effect of pressure on the final density tends to disappear. This is also relevant for process simulation.

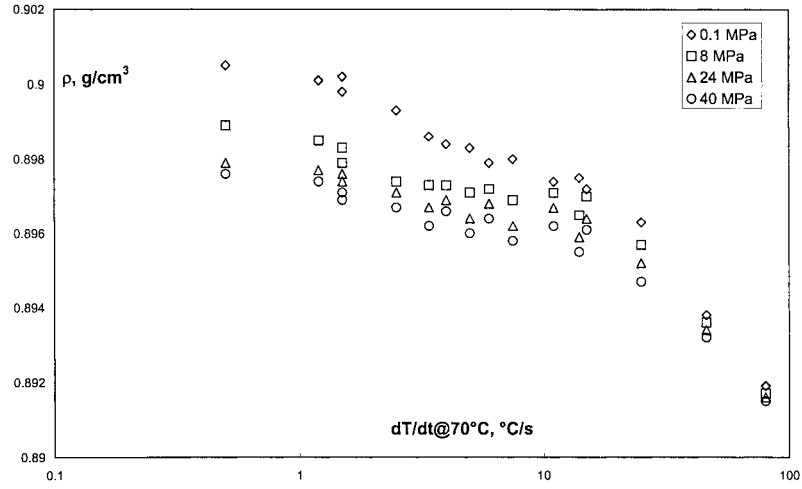

Fig. 5. Density versus calculated cooling rate for iPP

Fig. 5 is obtained by plotting the density data of figs. 1 and 2 versus the cooling rate calculated at 70°C by using a transient heat conduction model, as reported elsewhere [7-8]. The value of the calculated cooling rate was averaged across every slice thickness (50μm). The use of the transient model is also validated by the quite satisfactory overlapping of the data referred to a surface cooling rate of 100 and 20 °C/s. Also fig. 5 shows that at constant cooling rate final density decreases with pressure. Independently on solidification pressure the material shows the same trend with the cooling rate, with

a density drop above 10-20 °C/s. Finally, fig. 5 shows that the decrease of density with pressure vanishes with increasing cooling rate. This implies that the influence of pressure is more pronounced in the bulk of the sample, which is highly relevant in process simulation.

Also micro hardness results of fig. 4 were converted into the diagram shown in fig. 6, where micro hardness as a function of cooling rate is reported. In this case the local value of the calculated cooling rate was adopted.

A similar pressure dependence on the density has also been observed by *He and Zoller* [16] using a standard dilatometer by *GNOMIX Inc.* to measure sample specific volume during crystallization from the melt. A constant slow cooling rate (2-3 °C/min) under constant pressure was applied bringing the sample back to a fixed pressure at the end of the test (10 MPa). It is worth noticing that most experimental results provide the specific volume at the measurement pressure, whereas in our case we measure density at ambient pressure after solidification under pressure. *He and Zoller* observed an increase of specific volume with increasing crystallization pressure in the case of iPP while PA66 and PET show an opposite behaviour [16]. Although they tried to explain the density decrease with the formation of γ phase, which is less dense than α phase, in our samples there is no evidence of γ phase formation [7-9]. Their results re however in agreement with our results, where final density (measured at atmospheric pressure) of samples solidified under pressure turns out to be lower than the one of samples solidified at atmospheric pressure.

3.2 Density versus cooling rate for iPP from 0.01 to 100 °C/s, extension to low cooling rates

In order to extend the range of cooling rate to be explored below the minimum achievable cooling rate using the modified injection moulding machine (around 1°C/s), the already mentioned pressurized cell was used, completely different from the former as for the way of producing a constant pressure field during sample crystallization. In both experiments (modified injection moulding machine and pressurized cell) the same methodological approach of recording the thermal history experienced by the samples during cooling and then analysing the resulting sample morphology was adopted. Due to the small size and the low achievable maximum cooling rate (less than 2°C/s), the samples crystallized in the pressurised cell were completely homogeneous and their density was measured in a density gradient column.

Reporting all the data obtained using both apparatus, the density versus cooling rate (evaluated at 70°C) dependence shown in fig. 6 is obtained. It is worth reminding that the cooling rate was measured for samples crystallized in the pressurized cell, whilst for samples solidified in the modified injection moulding machine the cooling rate was calculated by means of a heat transfer model. The first result that must be emphasised is the good matching of data referred to completely different experimental set-up (fig. 6). As a matter of fact, the pressurised cell data obtained by solidification at 2°C/s (maximum achievable cooling rate with this apparatus due to the intrinsic constraints imposed by the heat transfer), indicated with open symbols, exhibit a satisfactory overlapping with the data obtained in the modified injection moulding machine, indicated with full symbols. This outcome confirms once more the reliability of the whole experimental route adopted, including the use of the simplified heat-transfer model to map the distance from the diaphragm with cooling rate [8].

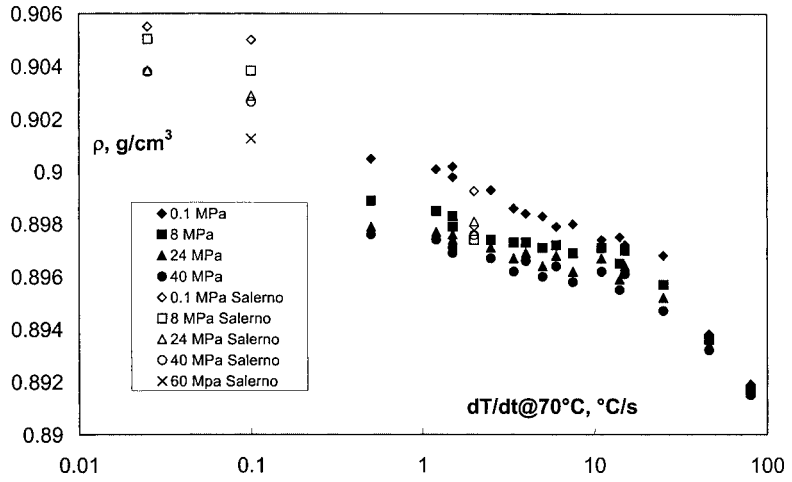

Fig. 6. Density versus cooling rate of samples prepared in the injection moulding machine (full symbols) and in the pressurised cell (open symbols)

The other experimental points achieved by means of the pressurised cell were at the cooling rates of 0.1 °C/s and 0.02°C/s (indicated with open symbols in fig. 6). The final density versus cooling rate dependence covers nearly four orders in magnitude in cooling rate (from about 0.01 up to nearly 100°C/s). Three regions can be distinguished within the diagram. A region of high cooling rates (higher than 20°C/s), characterised by a sharp fall in density, in this zone the role played by the solidification pressure is

almost negligible, since the density gap between 0.1 and 40 MPa is very small. In other words, in the high cooling rate region, the final density value is dominated by cooling rate, and it can be therefore considered to be independent on the pressure applied during the crystallisation process. In the second region, spanning from 1 to 20°C/s, density exhibits a gradual fall at all the investigated solidification pressures. Solidification pressure here strongly affects the final density value, the higher the pressure the lower the final density.

In this range of cooling rates it may be observed that a cooling rate increase has the same effect as an increase of pressure. On this basis the effect of pressure on the final density may be accounted for by using a "master curve" which reports density as a function of a so-called "equivalent cooling rate", correctly taking into account the real cooling rate and the additional shift caused by the solidification pressure [7]. The physical basis of this approach is that, across this zone, an increase of cooling rate at a constant pressure corresponds to an increase of pressure at a constant cooling rate in terms of final density and phase distribution (from WAXS). The third region corresponds to the low cooling rate zone, ranging from 0.01 to 1°C/s. A gradual decrease of density may be noticed with the same influence of solidification pressure on final density seen in the region 1-20°C/s. The effect of pressure on the final density may be accounted for by using a different master curve, determined on the basis of the experimental density data of this region. From fig. 6 it is also evident a sharp fall of density from 0.1 °C/s to 1°C/s at all the solidification pressures. This result together with the WAXS deconvolution data lead to the conclusion that a further process must occur when cooling rate becomes lower than 1°C/s. This process is responsible for the observed increase of density and alpha phase.

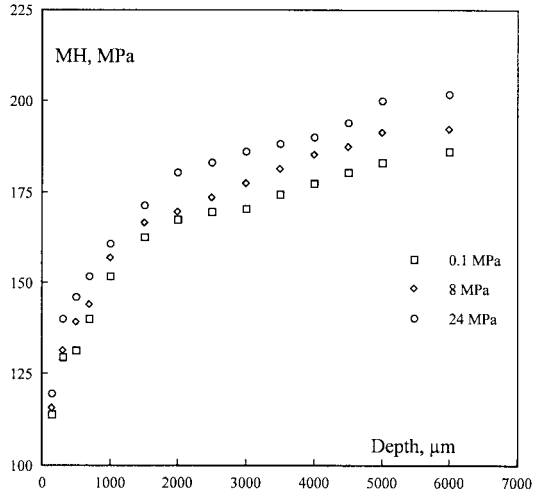

Fig. 7. Micro hardness versus depth (PET)

A "secondary crystallization" process in series to the first one may indeed give a plausible justification of density and WAXS results, as explained elsewhere [9].

3.3 Micro hardness and density measurements on PET samples

On PET samples it was not possible to measure the density variation by microtoming thin slices in the direction of sample thickness, due to the high brittleness of specimens which did non allow one to microtome them. Anyway it was possible measuring density of thick layer of polymer extracted from the bulk of the samples for all the adopted working pressures: 0.1, 8 and 24 MPa. Furthermore many density data of samples solidified under atmospheric pressure in a wide range of operating conditions are available. These measurements can lead to an indirect calculation of density data based on the densities of samples crystallized under ambient pressure conditions.

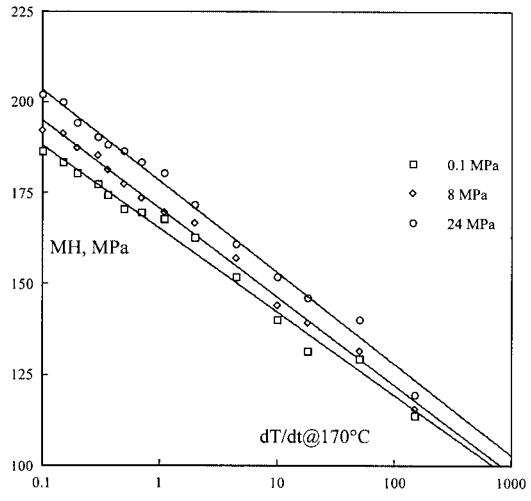

Fig. 8. Micro hardness versus cooling rate (PET)

On samples crystallized under pressure several micro hardness measurements were performed. A standard Vickers microindenter was used. A load of 100 g was applied for 6 s. with a loading velocity equal to 50 g/s. In this way a complete mapping of the sample was possible. Experimental results, in terms of micro hardness as a function of depth for all solidification pressures, are reported in fig. 7. First of all, as in the case of iPP, micro hardness increases going from the cooled surface to the bulk of the sample. In other words internal layers of polymer undergo a less severe quenching, which determines a lower value of crystallinity. This in turn causes micro hardness to increases on increasing depth, as shown in fig. 7.

As for dependence on pressure, PET displays an opposite behaviour with respect to the one exhibited by iPP (see fig. 4). As a matter of fact an increase of pressure corresponds

to an increase of MH. Any possible explanation of the different behaviour displayed by the two polymers should probably rely on the different chemical structure. For PET *Phillips and Tseng* [17] have found similar results on PET crystallized under pressures up to 200 MPa. They observed a reduction of the average spherulite size as pressure is increased, with a much greater effect than that observed in other studies on different polymers. A crystallinity level nearly double than the one obtained at atmospheric pressure was obtained at a pressure of 150 MPa. It appears from their results that the increase of density with pressure is a direct result of the applied pressure during crystallization, since PET is a polymer with a very rigid repeating unit. Probably the molecular flexibility could be the key to understand the different behaviour displayed by iPP and PET under pressure. Furthermore the present results are in agreement with the experimental results presented by *He and Zoller* [16], who found a significant increase of density with pressure for PET, in contrast with the decrease observed for iPP.

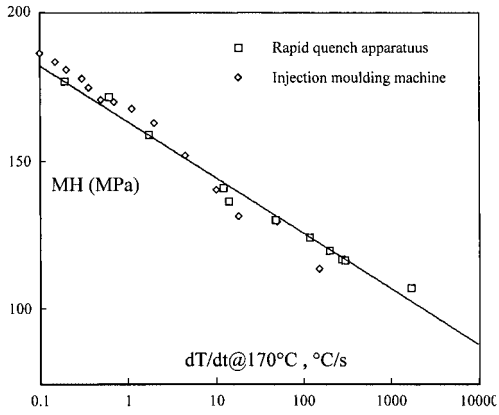

Fig. 9. Comparison between micro hardness data at 0.1 MPa obtained in different apparatus

From fig. 7, by using the "depth/cooling rate transformation function" for PET [9], calculated by using the heat transfer model, one can obtain data shown in fig. 8. In this figure micro hardness versus the calculated cooling

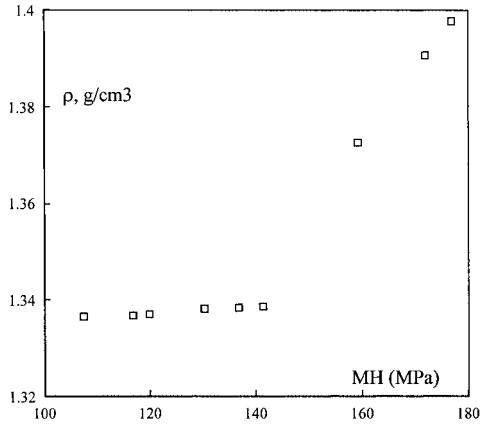

Fig. 10. Density versus micro hardness for samples obtained in the rapid atmospheric quench apparatus

rate (measured at 170°C) is plotted. Cooling rate is calculated at 170°C for PET since other works the past few years have demonstrated that this parameter is a good measure of quench effectiveness [5]. Fig. 8 shows that micro hardness decreases when the cooling rate increases. Furthermore, at a constant cooling rate, micro hardness increases with pressure in the whole cooling rate range examined. Finally micro hardness goes almost linearly with cooling rate (in a log scale) for all the solidification pressures.

It is interesting to compare micro hardness data of samples crystallized at ambient pressure in the apparatus developed for this work with micro hardness data of samples crystallized in a fast quenching ambient pressure apparatus developed by the authors few years ago. It is worth remembering that in the low pressure apparatus thin polymeric films (100 μm) are obtained and therefore the temperature profile inside the specimens is nearly flat. As a consequence of that, the cooling rate values are directly measured by using a thermocouple that records the thermal history. In our case the cooling rate is calculated by using the transient model. The comparison, shown in fig. 9, is quite satisfactory, demonstrating once again a good agreement between data obtained with the two different apparatus.

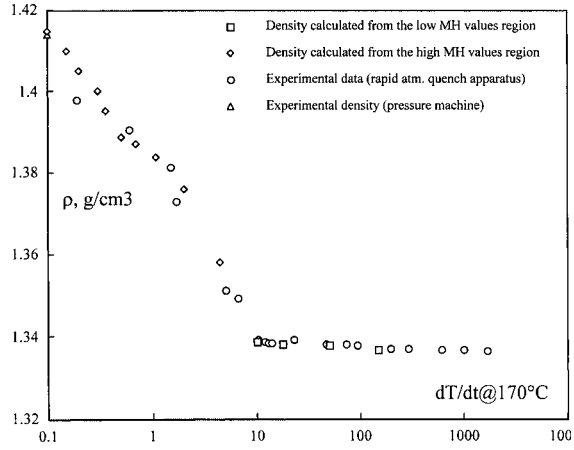

Fig. 11. PET. Comparison between experimental and calculated density (on the basis of micro hardness data)

Fig. 10 reports density versus MH for films obtained in the rapid quench apparatus at ambient pressure. In the low-density range, there is a significant increase of MH being the density nearly constant. Above micro hardness values of 140-150 MPa, the increase of micro hardness is accompanied by a parallel increase of density. This relationship between density and micro hardness can be described by using two different straight lines: ones in the low-density region and one (with an higher slope) in the high-density region. By using this analytical representation it is possible to calculate in an indirect way some density data. As a

matter of fact micro hardness data reported in fig. 8 can be transformed into density data, shown in fig. 11. In fig. 11 are also reported experimental density measurements of samples solidified in the low pressure quench apparatus. Experimental and calculated data are closed each other, the comparison being satisfactory. In the same figure there is also one experimental point at a cooling rate of 0.1 °C/s. This point refers to a density measure made on a thick slice extracted from the bulk of the sample crystallized at 0.1 MPa in our apparatus. The obtained vale is also in agreement with the other results.

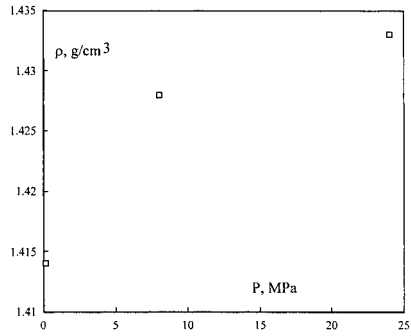

Fig. 12. PET density at 0.1 °C/s versus pressure

Finally fig. 12 shows density data for samples extracted from the bulk of samples crystallized under different pressure (having a cooling rate of 0.1 °C/s) as a function of solidification pressure. As a further proof of PET behaviour under pressure, density increases with pressure.

3.4 PA6 density and MH dependence upon cooling rate and pressure

Fig. 13 reports density of PA6 samples as a function of depth for all the adopted solidification pressures. Three different zones can be identified on that diagram. The first zone, near the cooled wall, is characterised by higher cooling rate values, and it could be easily noticed that density, going from the surface up to a depth of around 700 μm, remains nearly constant at a constant solidification pressure. Only a very small gap separates experimental densities of samples

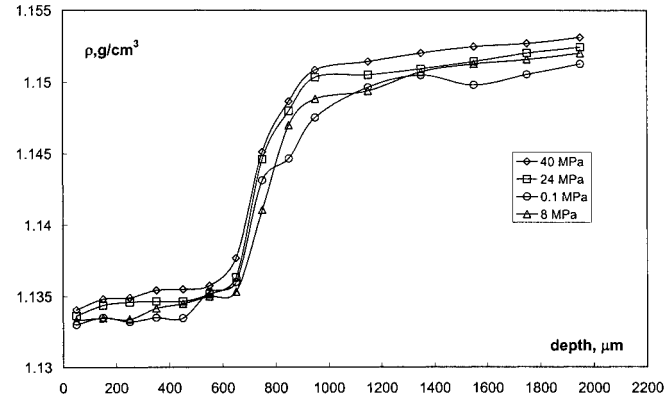

Fig. 13. PA6 Density depth profile

crystallised at ambient pressure with respect the ones crystallised under higher pressure conditions. Anyway the increase of density with increasing solidification pressure is not negligible. The second zone corresponds to a sort of "Transition zone" where the most significant variations of density versus depth take place. As a matter of fact, in the region where depth ranges from 700 μm up to 1000 μm, a sudden rise of density should be pointed out, independently on the working solidification pressure. In the whole transition zone the effect of pressure on the final sample densities turns out to be negligible. Finally, the third region, the "bulk zone", starting from a depth of approximately 1000 μm, it is the region where density tends to level off with increasing depth for a given solidification pressure. The effect of solidification pressure on the final density across this zone appears to be more pronounced than in the low-density plateau. Specifically, the higher the pressure the higher the resulting final density. On the whole, the increase of density due to the increase of solidification pressure is of the same order of magnitude of the decrease of density observed in the case of iPP, as already discussed above. This evidence turns out to be in full agreement with the dilatometric results reported by *He and Zoller* in 1997 [16], who found a decrease of density with solidification pressure of 0.1% in the case of iPP, while they noticed an increase of density of 0.3% in the case of PA66. It should be remembered that the cooling rate adopted during their experiments was very low (1-2°C/min) due to the intrinsic constraints imposed by the apparatus [16].

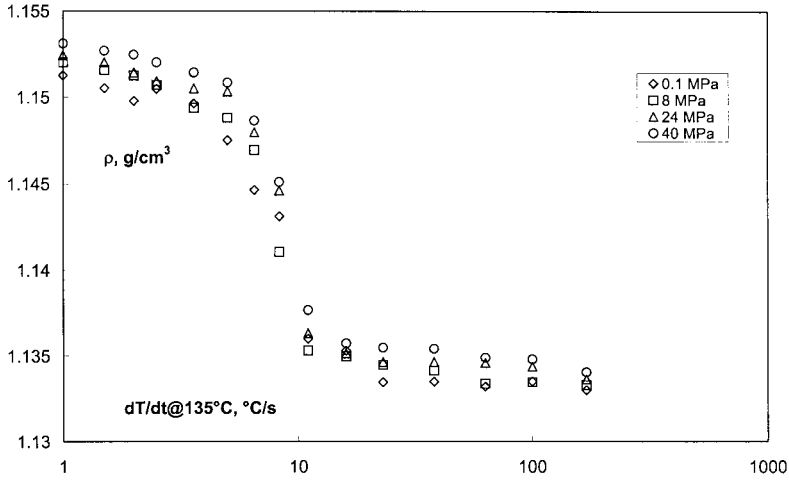

Fig. 14. PA6 density versus cooling rate evaluated at 135°C

If density of PA6 is reported as a function of cooling rate measured at 135°C [4] by means of the "depth-cooling rate mapping function" [9], the same trend discussed above is observed, as it could be noticed by looking through fig. 14. The low-density plateau corresponds to the high cooling rate region, and its starting point is located above 10°C/s. This region covers more than one order of magnitude in cooling rates, reaching the cooling rate of 250°C/s. The high-density plateau covers nearly one order of magnitude in cooling rate, going from the lowest achieved cooling rate during the experiment (1°C/s) up to 7-8 °C/s. As for the transition zone, it should be pointed out that it is located in a very narrow region, centred at a cooling rate of about 8-10°C/s. This cooling rate could be defined as a sort of "critical cooling rate" since small changes of cooling rate around this value could determine large structural and morphological variations that, in turn, determine large density variations. A very similar value of critical cooling rate was already found for a different PA6 some years ago, which is in agreement with the results here presented [4]. This value corresponds to the so-called "crystallizability" value defined by *Ziabicki* several years ago [18].

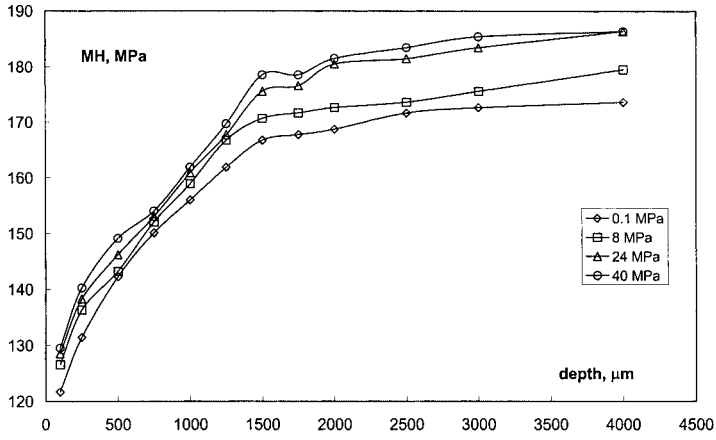

Fig. 15. PA6 micro hardness depth profile

As far as the micro hardness behaviour of PA6 is concerned, a different sensitivity with respect to the density behaviour is to be highlighted. Fig. 15 reports MH of PA6 samples as a function of depth for all the adopted solidification pressures. The first evidence to be analysed is a continuous gradual raise of micro hardness with depth, starting form the cooled wall. In other words, the low-density plateau, observed in the case of density, does not show up for micro hardness. A second issue concerns the high

micro hardness plateau value. As a matter of fact this plateau corresponds only partially to the one observed in density, since its starting point is located at a much larger depth, around 1500 μm. All these differences could be explained by taking into account that density is a material "bulk" property, while micro hardness is a "surface" property and for this reason the latter turns out to be much more sensitive to any structural modification than the former. The reader should remember that a similar comparison was made in the case of iPP, where the structural and morphological modifications at the cooled wall can be easily highlighted by measuring the micro hardness profile (fig. 4), while in the case of density the variations measured near the surface were much less evident (figs. 1 and 2). As for the influence of pressure on the final micro hardness values, fig. 15 shows that an increase of pressure determines a parallel increase of micro hardness in the whole explored depth. Nevertheless the effect of pressure is more remarkable in the internal region of samples (in the high micro hardness plateau zone), where the gap between low pressure and high pressure crystallised samples tends to broaden. When Micro Hardness is reported as a function of cooling rate (fig. 16), the value of cooling rate above which the increase of micro hardness due to the increase of pressure turns out to be less pronounced, could be identified. This last corresponds to a cooling rate of about 5-6 °C/s lower than the critical value (8-10°C/s) found in the case of density.

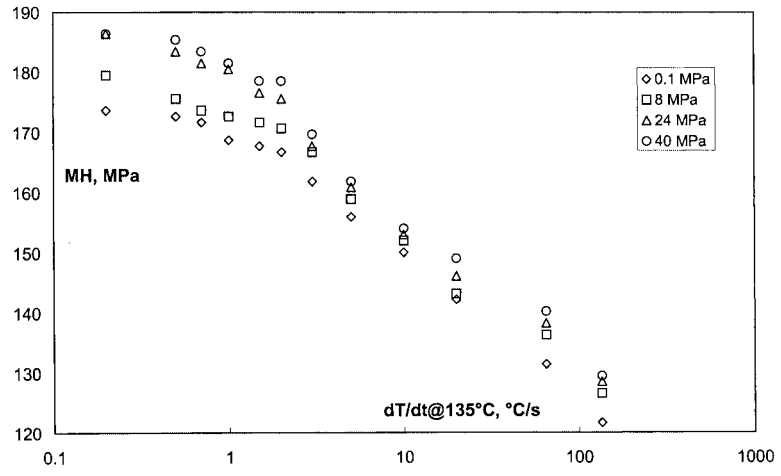

Fig. 16. PA6 micro hardness versus cooling rate evaluated at 135°C

References

[1] S. Piccarolo, *J. Macromol. Sci. – Phys. B*, **1992**, *31*, 501.

[2] S. Piccarolo, M. Saiu, V. Brucato, G.Titomanlio, *J. Appl. Poly. Sci.*, **1992**, *46*, 625.

[3] V. Brucato, T. Foresta, S. Piccarolo, *Proc. of NUPHIMAT'96*, **1996**, p.125.

[4] V. Brucato, S. Piccarolo, G. Titomanlio, *Int. Jou. of Forming Processes*, **1998**, *1*, 35.

[5] S. Piccarolo, V. Brucato, Z. Kiflie, *Polym. Eng. and Sci.*, **2000**, *40*, 1263.

[6] V. Brucato, G. Crippa, S. Piccarolo, and G. Titomanlio, *Polymer Eng. and Sci*, **1991**, 31.

[7] V. La Carrubba, V. Brucato, S. Piccarolo, *Polym. Eng. And Sci.*, **2000**, *40*, 11.

[8] V. Brucato, S. Piccarolo, V. La Carrubba, *Int. Polym. Proc.*, **2000** *15*, 103.

[9] V. La Carrubba, *"Polymer solidification under pressure and high cooling rate", Ph.D. Thesis*, CUES, Salerno 2000.

[10] G. Hitchcock, V. Brucato, S. Piccarolo, *Proc. of PPS12- Twelfth International Annual Meeting of the PPS*, **1996**, p.701.

[11] V. La Carrubba, *Thesis in Chemical Engineering*, University of Palermo, 1997.

[12] A. Martorana, S. Piccarolo, F. Scichilone, *Macromol Chem. Phys.*, **1997**, *198*, 597.

[13] G. Titomanlio, V. Speranza, V. Brucato, *Int. Polym. Proc.*, **1997**, *12*, 45.

[14] G. Titomanlio, S. Piccarolo, G. Levati, *Jou of Appl. Polym. Sci.*, **1988**, *35*, 1483.

[15] G. Titomanlio, A. Rallis, S. Piccarolo, *Polym. Eng. And Sci.*, **1988**, *29*, 209.

[16] J. He and P. Zoller, *J. Polym. Sci., Part B*, **1994**, *32*, 1049.

[17] P. J. Phillips, and H. T. Tseng, *Macromolecules*, **1989**, *22*, 1649.

[18] A. Ziabicki, *"Fundamentals of Fibre Formation"*, Wiley, London 1976.